

To: Mr. Chas. J. McCarthy
THIS DOCUMENT AND EACH AND EVERY
PAGE HEREIN IS HEREBY RECLASSIFIED
FROM Conf TO Unclass
AS PER LETTER DATED NACA, Dec 1965.
Notice # 122

74
Source of Acquisition
CASI Acquired

NATIONAL ADVISORY COMMITTEE FOR AERONAUTICS

SPECIAL REPORT No. 98

INTERFERENCE OF TAIL SURFACES AND WING AND FUSELAGE
FROM TESTS OF 17 COMBINATIONS IN THE N.A.C.A.
VARIABLE-DENSITY TUNNEL

By Albert Sherman
Langley Memorial Aeronautical Laboratory

January 1939

SR-98

INTERFERENCE OF TAIL SURFACES AND WING AND FUSELAGE

FROM TESTS OF 17 COMBINATIONS IN THE N.A.C.A.

VARIABLE-DENSITY TUNNEL

By Albert Sherman

SUMMARY

An investigation of the interference associated with tail surfaces added to wing-fuselage combinations was included in the interference program in progress in the N.A.C.A. variable-density tunnel. ⁽¹⁾The results indicate that, in aerodynamically clean combinations, the increment to the high-speed drag can be estimated from section characteristics within useful limits of accuracy. ⁽²⁾The interference appears mainly as effects on the downwash angle and as losses in the tail efficiency and varies with the geometry of the combination. ⁽³⁾An interference burble, which markedly increases the glide-path angle and the stability in pitch before the actual stall, may be considered a means of obtaining satisfactory stalling characteristics for a complete combination.

INTRODUCTION

The investigation that the Committee has been conducting in the variable-density wind tunnel of the aerodynamic interference between the wing and the fuselage (references 1 to 6) has been extended to include the interference associated with the tail surfaces. Comparable data at large scale are thus made available on the aerodynamic interference between the component parts of related complete combinations.

Representative wing-fuselage combinations were tested, to which had been added two different types of tail surfaces: conventionally arranged tail surfaces of semi-elliptical plan form and rectangular horizontal tail surfaces with elliptical end plates. The tests were restricted to the conditions of zero elevator deflection and zero yaw, and the effects of the interference on the drag, the downwash angle, and the tail efficiency were mainly considered. Effects of the following variables on the interference of the tail surfaces were studied: wing position, angle of wing setting, form of tail surface, and form of

wing-root juncture. A comparison of calculated and experimental data on the downwash angle at the tail is also included.

MODELS AND TESTS

The wing employed is the tapered wing described in reference 1; it is a duralumin model having an area of 150 square inches, aspect ratio 6, taper ratio 2, and the N.A.C.A. 0018 section at the root and the N.A.C.A. 0009 section at the tip. It was combined with the fuselage in the standard longitudinal position, $d/c = 0$. The fuselage is the round fuselage described in reference 1; it is an airship form having a length of 20.156 inches and a fineness ratio of 5.86. The tapered fillets (reference 1) were carefully constructed of plaster of paris and were given the polished lacquer finish now standard for the wing-fuselage-interference investigation (reference 5). Figures 1, 2, and 3 are photographs of interesting combinations and show the proportions of the tail surfaces and their location on the fuselage axis.

The details of the tail surfaces are given in figure 4. For the elliptical tail surfaces, the vertical surface is identical with each of the horizontal surfaces. The tail with end plates has approximately the same total wetted area as the elliptical horizontal and vertical tail surfaces, but its calculated total-lift-curve slope was predicted from the theory of reference 7 to be 84 percent as large. Only very small fillets were used at the tail surfaces (see figs. 1 and 2) because filleting was believed unnecessary for the junctures employed. The test results do not indicate that larger fillets would be an improvement. Table V contains the descriptions of the combinations (314 to 330) that make up this investigation.

The combinations were tested in the variable-density wind tunnel (reference 8) at a test Reynolds Number of approximately 3,100,000, corresponding to an effective Reynolds Number for $C_{L_{max}}$ of 8,200,000. (See reference 1.) In addition, values of the maximum lift coefficient were obtained at a reduced speed corresponding to an effective Reynolds Number of 3,700,000. The testing procedure and the test precision were about the same as for an airfoil (reference 8). The three-component balance of the variable-density wind tunnel restricted the study of the vertical tail surfaces to the zero-yaw condition.

RESULTS

The test results are given in tables I, II, III, IIIa, and V supplemented by figures 5 to 10. Data from previous reports are included for comparison. Additional derived data on tail efficiency and downwash angle at the tail are presented in the text of the discussion and in figure 11. The aerodynamic characteristics are given as standard non-dimensional coefficients based on the projected wing area of 150 square inches and on the mean chord of 5 inches. The methods for analysis of the test data and for presentation of the test results are explained in reference 1.

Tables I and II, taken from reference 1, contain the aerodynamic characteristics of the wing and of the fuselage, respectively. Table III, continued from reference 6, presents the sums of the fuselage characteristics and interferences (ΔC_L , ΔC_{D_e} , $\Delta C_{m_c}/4$) for the different combinations at various angles of attack. Table IIIa, continued from reference 6, presents the sums of the characteristics and interferences of the tail surfaces. The characteristics of the combinations themselves can be determined by adding the corresponding items in tables I, III, and IIIa.

Table IV of reference 1, which presents the data for disconnected combinations (combinations for which the forces on the components are measured separately), is omitted herein as it is in references 2 to 6 because no further tests of this nature were performed. The table numbers are maintained as in reference 1, however, to preserve the continuity of the published test results of the interference investigation.

Table V, continued from reference 6, contains the principal geometric and aerodynamic characteristics of the combinations. The values d/c and k/c represent the longitudinal and the vertical displacements, respectively, of the wing quarter-chord axis measured (in mean chord lengths) positive ahead of and above the quarter-length point of the fuselage axis. The value i_w is the angle of wing setting with respect to the fuselage axis and i_s is the setting of the tail surfaces relative to the wing.

The last nine columns of table V present the following important aerodynamic characteristics:

a, lift-curve slope (in degree measure) as determined in the range of low lift coefficients for an effective aspect ratio of 6.86. This value of the aspect ratio differs from the actual value for the models because the lift results are not otherwise corrected for tunnel-wall interference.

e, Oswald's airplane, or span, efficiency factor. (See reference 1.)

$C_{D_{\min}}$, minimum effective profile-drag coefficient
 $\left(C_D - \frac{C_L^2}{\pi A}\right)_{\min}$ corresponding to the test Reynolds Number.

$C_{L_{\text{opt}}}$, optimum lift coefficient, i.e., the lift coefficient corresponding to $C_{D_{\min}}$. For the combinations with tail surfaces, however, the lift at an arbitrary angle of trim, i.e., where $C_{m_c/4} = 0$, is given instead.

n_o , aerodynamic-center position, indicating approximately the location of the aerodynamic center ahead of the wing quarter-chord axis as a fraction of the mean wing chord. Numerically, n_o equals $dC_{m_c/4}/dC_L$ at zero lift. For the combinations with tail surfaces, however, n_o is given instead for the arbitrary trim condition, i.e., $C_{m_c/4} = 0$.

C_{m_0} , pitching moment at zero lift.

$C_{L_{\text{lib}}}$, lift coefficient at the interference burble, i.e., the value of the lift coefficient beyond which the air flow has a tendency to break away as indicated by an abnormal drag increase.

$C_{L_{\max}}$, maximum lift coefficient given for two different values of the effective Reynolds Number. (See reference 1.) The turbulence factor employed in this report to obtain the effective R from the test R is 2.64.

As in reference 2, the values of the effective Reynolds Number differ somewhat from those given in reference 1 because of a later determination of the turbulence factor for the tunnel. The values of the effective Reynolds Number given in reference 1 can be corrected by multiplying by 1.1.

The data thus presented for the combinations with tail surfaces are directly applicable to design purposes only at the attitude for trim, that is, when the pitching moment about the center of gravity is zero. At other attitudes, the conditions of the tests cannot be reproduced in steady flight. The most important interference effects for tail surfaces, however, should be satisfactorily indicated over the range of lift coefficients by these results.

DISCUSSION

Lift

The horizontal tail surfaces add to the lifting area of a combination and should therefore increase the lift-curve slope and the maximum lift. For the combinations tested, the gain in lift-curve slope amounted, within the limits of the test accuracy, practically to the value that would be calculated from the lift expected of the tail operating alone as a wing, the downwash and the wake interferences being neglected. The observed increases in the maximum lift (table V) naturally cannot be considered real as they were obtained with undeflected elevators and highly unbalanced pitching moments. The effect on the maximum lift of the interference of tail surfaces with elevators deflected is outside the scope of this investigation.

Drag

The experimental increments to the minimum drag coefficients of the combinations due to the semielliptical tail surfaces at 0° setting (0.00035 to 0.00055 per surface) agree within the test accuracy with a value estimated from section characteristics and the wetted area (0.00045 per surface). This agreement shows that no large resultant interference effect of the tail surfaces could have been present. The horizontal tail surfaces set $\pm 4^\circ$ show larger contributions to the minimum drag than those set 0° , but

the differences are generally too small to be important. (See table V.)

Over the range of low to moderate lift coefficients, the variation in the drag increment also was unimportant for two of the tail settings investigated (0° and -4°) and, moreover, was often favorable (figs. 5, 6, and 7). For a tail setting of 4° , however, this variation was appreciable and adverse.

From the foregoing considerations it can be concluded that, with regard to the high-speed or cruising drag, cleanly constructed tail surfaces within the normal range of tail settings may be satisfactorily allowed for in design by simple calculations based on section characteristics and the wetted area, neglecting interferences. Incidentally, the data indicate how low a drag should be expected from cleaning up the conventional airplane design. The value of 0.0135 ($R = 3 \times 10^6$) for the effective profile-drag coefficient for combinations 314 and 315 (fig. 5) at a C_L of about 0.3 represents the drag obtainable for a small airplane. In view of the turbulence present in the air stream of the variable-density wind tunnel and the unevaluated part of the support-strut interference, this value is believed to be conservative. Extrapolation of the drag values given in this report to higher Reynolds Numbers can be made by the methods described in reference 9.

Pitching Moment

The horizontal tail surfaces are employed to provide stability in pitch. They form what is essentially an airfoil operating under the influence of an interfering body, the wing-fuselage combination. The most important interferences at the tail may be separated into two effects: that on the flow direction, or the downwash; and that on the flow velocity, or the wake.

Downwash.— When the wing-fuselage combination is lifting, the downflow components induced by the vortex pattern in the air stream reduce the effective angle of attack at the tail by an amount referred to as the "downwash angle" ϵ .

The evaluation of ϵ is necessary in stability calculations. A method exists for the prediction of the downwash angle at the tail associated with any type of wing.

(reference 10), but the amount that ϵ is modified by the interference in a wing-fuselage combination remains to be found. Figure 11 gives a comparison of values of the average downwash angle over the tail span as calculated by the method of reference 10 and as derived from the experimental results for the elliptical tail surfaces on the high-wing, the midwing, and the low-wing combinations. Experimental values of ϵ for the tail with end plates are included for the midwing combination. The method employed to obtain the experimental values was as follows: At each specified angle of attack, the rate of change of pitching moment with the angle of attack of the tail was determined from the pitching moments for tail settings of -4° , 0° , and 4° . Next, the change produced in the pitching moment by adding the tail surfaces was divided by the rate just derived to give the effective angle of attack of the tail. The experimental value of the downwash angle ϵ , then, was the difference between the geometric angle of attack of the tail and its effective angle of attack. This procedure avoided the complications of the wake interference and the tail efficiency.

It can be seen from figure 11 that, for the elliptical tail on the symmetrical midwing combination, the agreement between the predicted and the experimental downwash angles is good over the range of low to moderate lift coefficients. Apparently, the interference of the fuselage and the junctures was negligible. For the high-wing and the low-wing combinations the agreement is poor. The discrepancy, however, is practically constant, therefore of little importance in stability calculations, and is of opposite sign for the high-wing and the low-wing combinations. Apparently, at zero lift the tail surfaces have already an initial effective angle of attack of approximately 0.8° for the low-wing and -0.8° for the high-wing combinations. (See pitching-moment curves of figs. 6, 7, and 8.) The geometrical asymmetry, then, produces an initial deviation in the flow at the tail impossible to derive from a theory that considers only the wing. A comparison of figures 7 and 9 shows that most of this interference is chargeable to the fillets. The same effect can be produced, however, by other sources of asymmetry, such as wing setting. (Cf. curves of pitching moment in fig. 10, and also C_{m_0} for combinations 314 and 322 in table V.)

Figure 5 shows that, for zero tail setting and at low to moderate lift coefficients, the tail surfaces with end

plates produce as large a change in the pitching moment as the elliptical tail surfaces, indicating that they should have as high a slope of the total-lift curve. The slope for the end-plate tail, however, has been calculated to be only 84 percent of that for the elliptical tail. This calculation appears corroborated, moreover, by the change in the pitching moment at zero lift developed by the end-plate tail, corresponding to a change from 0° to -4° in tail setting, which was also about 84 percent of the change produced by the elliptical tail (fig. 5). The apparent inconsistency may be explained by the experimental, and unexpected, circumstance that the average downwash angle affecting the end-plate tail was slightly less than that affecting the elliptical tail and balanced its lower lift-curve slope. (See fig. 11. Refer also to pitching-moment curves in fig. 5.) No explanation for this difference in downwash is offered. Further investigation of tail surfaces of different geometrical characteristics may provide a better understanding of the nature of such interference phenomena.

Stability at the stall.— The problem of obtaining satisfactory stalling characteristics is again commanding attention in connection with the refined present-day monoplanes. An essential feature of a satisfactory stall is that it give ample warning, associated preferably with rapidly increasing stability in pitch. Figure 9 presents the aerodynamic characteristics for a low-wing unfilleted combination of moderate aspect ratio (see fig. 3) that employs a common method of achieving such a stall, an interference burble (see reference 1); the burble occurred at a lift coefficient of about 1.0, which is above the climbing range, and resulted in a loss of downwash at the tail. As the angle of attack was increased, the lift continued to increase slowly to the maximum but the diving moment and the drag rose precipitously, insuring a steeper glide path, an appreciable increase in stability in pitch, and thus a warning of the approaching stall. It is understood from flight results that some tail buffeting may occur simultaneously; this buffeting is an unmistakable warning that cannot be overlooked. The interference burble can be delayed to a higher lift coefficient, if so desired, and the cost in maximum lift and minimum drag can be reduced by small fillets. The use of the interference burble is therefore not necessarily a makeshift solution in the design of airplanes for acceptable stalling characteristics.

Tail efficiency.— The tail efficiency, η_t , may be

defined as the ratio of experimental to calculated changes in the pitching moment due to the horizontal tail surfaces. The calculated changes may be derived from the geometric and the aerodynamic characteristics of the tail surfaces, with due allowance for the downwash angle and the flow velocity at the tail as affected by the wake. Ordinarily, the efficiency is derived from the experimental and the calculated changes in the pitching moment of the combination produced by different settings of the tail surfaces for a given angle of attack of the wing. This procedure avoids the complications involved with the downwash angle at the tail. Such a derivation results, however, in an efficiency corresponding to a varying angle of tail setting rather than one for a varying angle of attack of the combination as a whole. The interferences associated with various tail-surface settings might possibly differ, and hence the efficiency as ordinarily obtained would not strictly apply to stability calculations for which the tail changes angle together with the combination. As will be shown later, however, the variation in tail efficiency over a moderate range of angles of tail setting is generally unimportant for combinations such as reported herein.

If the tail efficiency is derived as described, it will differ from 100 percent by an amount proportional to the unevaluated interference. Reference 10 contains methods of obtaining the interference behind the wing. The interference with a fuselage present remains to be investigated. The following table presents a comparison of tail efficiencies for various combinations with allowance made for the interference of the wing alone in accordance with the methods of reference 10.

Notice that η_t is practically constant for the symmetrical midwing combinations over the range of angles of attack investigated. For the high-wing and the low-wing combinations, the efficiency shows greater amounts of unevaluated interference at low angles of attack than for the midwing combination. Most of the difference is believed to result from the asymmetry introduced by the fillets. (Notice in fig. 9 the reduction of slope in the pitching-moment curve associated with the fillets.) It appears, therefore, that a knowledge of the interference behind a wing alone is not sufficient for calculating the effectiveness of tail surfaces in combinations. Until further research more fully evaluates the interference at the tail of combinations, estimates based upon test results, such as in this report, must be relied upon in stability calculations.

COMPARISON OF TAIL EFFICIENCY FOR DIFFERENT WING-FUSELAGE COMBINATIONS

Combina- tion	k/c	i_w (deg.)	i_s (deg.)	Tail efficiency, η_t (averaged for $i_s=0^\circ$ to $\pm 4^\circ$)			$\Delta \left(\frac{dC_{mC}/4}{dC_L} \right)$ due to tail surfaces		
				$\alpha=0^\circ$	$\alpha=4^\circ$	$\alpha=12^\circ$	$\alpha=0^\circ$	$\alpha=4^\circ$	$\alpha=12^\circ$
Elliptical tail surfaces									
314	0	0	0	0.90 .77	0.91 .78	0.91 .65	-0.128	-0.157	-0.202
315	0	0	-4				-.127	-.146	-.196
327	0.22	0	4	0.79	0.82	0.90	-0.164	-0.198	-0.221
^a 312	.22	0	0	.79 .81	.82 .82	.90 .90	-.162	-.179	-.219
326	.22	0	-4						
330	-0.22	0	4	0.81	0.81	0.90	-0.168	-0.146	-0.191
^a 313	-.22	0	0	.81 .79	.81 .79	.90 .84	-.160	-.151	-.158
328	-.22	0	-4						
Tail surfaces with end plates									
316	0	0	0	0.92 .95	0.89 .96	0.89 1.04	-0.132	-0.160	-0.164
317	0	0	-4				-.143	-.150	-.157

^aFrom reference 6.

$\Delta \left(\frac{dC_L}{dC_L} \right) = \eta_t$ based on $\left(\frac{dC_L}{dC_L} \right)$ incl. tail and end plates

$$\left(\frac{dC_L}{dC_L} \right) \eta_t = A$$

The values of η_t given are obviously averages for the two tail settings employed in each derivation. For any combination chosen, at a specified angle of attack, the downwash angle and the wake interference may be assumed unchanged for various tail settings. Under such conditions, a variation in the change produced in the slope of the pitching-moment curve by adding tail surfaces

$\Delta \left(\frac{dC_{mc}/4}{dC_L} \right)$ is a direct indication of a variation in the tail efficiency. From the columns of $\Delta \left(\frac{dC_{mc}/4}{dC_L} \right)$ in the preceding table, it can be concluded that the tail setting did not, in general, greatly affect the tail efficiency at the lower lift coefficients within the range investigated and within the accuracy of the data. It appears, therefore, that an efficiency derived from a small range of tail settings is reasonably applicable to horizontal tail surfaces that change angle together with the combination as a whole. Check calculations with the data using efficiencies so derived corroborated this conclusion by correctly predicting the curves of pitching moment produced by the tail surfaces.

The efficiencies of the tail with end plates in the symmetrical midwing combination are practically the same as those of the elliptical tail. (Cf. also values of

$\Delta \left(\frac{dC_{mc}/4}{dC_L} \right)$.) This agreement indicates that the unevaluated interference is not intimately connected with the geometry of the tail surfaces themselves.

CONCLUSIONS

The results of the present tests show that:

1. The increment to the drag in the high-speed range caused by adding tail surfaces in the normal range of tail settings to clean combinations can be estimated within useful limits of accuracy from section characteristics and the wetted area, the interference being neglected.

2. The interference of the fuselage in symmetrical midwing combinations on the downwash angle behind the wing is small.

3. The effect of asymmetry in the combination is to introduce a corresponding initial deviation in the air stream at the tail.

4. The effective downwash angle at the tail may vary somewhat with the geometry of the tail surfaces under consideration.

5. An interference burble for a combination of wing, fuselage, and tail surfaces may be considered a satisfactory means of producing acceptable stalling characteristics.

6. For combinations such as were investigated, large fillets at the tail-surface junctures are unnecessary.

7. Knowledge of the interference behind the wing alone is not sufficient for evaluating the effectiveness of tail surfaces added to wing-fuselage combinations.

8. Tail efficiencies derived experimentally from small ranges of tail settings, the angle of the combination being held constant, can be considered to apply reasonably well to tail surfaces that change angle together with the combination as a whole.

Langley Memorial Aeronautical Laboratory,
National Advisory Committee for Aeronautics,
Langley Field, Va., November 5, 1938.

REFERENCES

1. Jacobs, Eastman N., and Ward, Kenneth E.: Interference of Wing and Fuselage from Tests of 209 Combinations in the N.A.C.A. Variable-Density Tunnel. T.R. No. 540, N.A.C.A., 1935.
2. Sherman, Albert: Interference of Wing and Fuselage from Tests of 28 Combinations in the N.A.C.A. Variable-Density Tunnel. T.R. No. 575, N.A.C.A., 1936.
3. Sherman, Albert: Interference of Wing and Fuselage from Tests of 30 Combinations in the N.A.C.A. Variable-Density Tunnel. Combinations with Triangular and Elliptical Fuselages. T.R. No. (to be published), N.A.C.A. 5865
4. Sherman, Albert: Interference of Wing and Fuselage from Tests of 18 Combinations in the N.A.C.A. Variable-Density Tunnel. Combinations with Split Flaps. T.N. No. 640, N.A.C.A., 1938.
5. Sherman, Albert: Interference of Wing and Fuselage from Tests of 17 Combinations in the N.A.C.A. Variable-Density Tunnel. Combinations with Special Junctionures. T.N. No. 641, N.A.C.A., 1938.
6. Sherman, Albert: Interference of Wing and Fuselage from Tests of Eight Combinations in the N.A.C.A. Variable-Density Tunnel. Combinations with Tapered Fillets and Straight-Side Junctionures. T.N. No. 642, N.A.C.A., 1938.
7. von Kármán, Th., and Burgers, J. M.: Single Wing with Shields at Ends. Vol. II, div. E, sec. 19 of Aerodynamic Theory, W. F. Durand ed., Julius Springer (Berlin), 1935, pp. 211-212.
8. Jacobs, Eastman N., and Abbott, Ira H.: The N.A.C.A. Variable-Density Wind Tunnel. T.R. No. 416, N.A.C.A., 1932.
9. Jacobs, Eastman N., and Sherman, Albert: Airfoil Section Characteristics as Affected by Variations of the Reynolds Number. T.R. No. 586, N.A.C.A., 1937.
10. Silverstein, Abe, and Katzoff, S.: Design Charts for Predicting Downwash Angles and Wake Characteristics behind Plain and Flapped Wings. T.R. No. 648, N.A.C.A., 1939.

TABLE I - Airfoil Characteristics

Airfoil	C_L	C_{D_e}	$C_{m_{c/4}}$	C_L	C_{D_e}	$C_{m_{c/4}}$	C_L	C_{D_e}	$C_{m_{c/4}}$
	$\alpha = 0^\circ$			$\alpha = 4^\circ$			$\alpha = 12^\circ$		
Tapered N.A.C.A. 0018-09	0.000	0.0093	0.000	0.305	0.0099	0.006	0.910	0.0146	0.013

TABLE II - Fuselage Characteristics

Fuselage	Engine	C_L	C_D	$^1C_{m_F}$	C_L	C_D	$^1C_{m_F}$	C_L	C_D	$^1C_{m_F}$	C_L	C_D	$^1C_{m_F}$	C_L	C_D	$^1C_{m_F}$
		$\alpha = 0^\circ$			$\alpha = 4^\circ$			$\alpha = 8^\circ$			$\alpha = 12^\circ$			$\alpha = 16^\circ$		
Round	None	0.000	.0041	.000	.001	.0042	.016	.005	.0049	.028	.011	.0062	.035	.019	.0085	.038

¹ Pitching-moment coefficient about the quarter-chord point of the fuselage.

TABLE III - Lift and Interference, Drag and Interference,
and Pitching Moment and Interference of
Fuselage in Wing-Fuselage Combinations

Com- bi- na- tion	ΔC_L	ΔC_{D_e}	$\Delta C_{m_{c/4}}$	ΔC_L	ΔC_{D_e}	$\Delta C_{m_{c/4}}$	ΔC_L	ΔC_{D_e}	$\Delta C_{m_{c/4}}$
	$\alpha = 0^\circ$			$\alpha = 4^\circ$			$\alpha = 12^\circ$		
230	0.003	0.0024	-0.003	0.023	0.0024	0.003	0.042	0.0040	0.012
319	-0.016	.0024	-0.023	-0.001	.0025	-0.019	.030	.0040	-0.009
321	-0.020	.0028	-0.022	-0.004	.0027	-0.016	.019	.0035	-0.002
306	.008	.0029	-0.001	.019	.0033	.003	.044	.0059	.012
307	-0.008	.0029	.001	.013	.0028	.005	.037	.0044	.011
308	-0.017	.0025	.009	-0.011	.0027	.017	-0.004	.0052	.032
309	.017	.0025	-0.009	.036	.0027	-0.004	.046	.0047	.006
187	.009	.0031	-0.008	.026	.0036	-0.001	.029	.0069	.010

TABLE IIIa - Lift and Interference, Drag and Interference,
and Pitching Moment and Interference of Tail
Surfaces in Combinations

Com- bi- na- tion	ΔC_L	ΔC_{D_e}	$\Delta C_{m_c/4}$	ΔC_L	ΔC_{D_e}	$\Delta C_{m_c/4}$	ΔC_L	ΔC_{D_e}	$\Delta C_{m_c/4}$
	$\alpha = 0^\circ$			$\alpha = 4^\circ$			$\alpha = 12^\circ$		
310	0.005	0.0011	0.009	0.030	0.0012	-0.050	0.097	0.0025	-0.190
311	-.005	.0011	-.009	.022	.0015	-.062	.078	.0041	-.166
312	-.003	<u>.0007</u>	.020	.027	.0008	-.037	.083	.0015	-.172
313	.003	<u>.0007</u>	-.020	.027	.0014	-.073	.061	.0038	-.171
314	.015	.0011	.003	.033	.0015	-.043	.097	.0046	-.167
315	-.035	.0018	.107	-.007	.0010	.063	.046	.0006	-.052
316	.015	.0014	.003	.037	.0017	-.046	.091	.0031	-.152
317	-.019	.0019	.088	.009	.0013	.040	.054	.0010	-.058
318	-	-	-	-	-	-	-	-	-
320	.003	.0015	-.010	.033	.0015	-.059	.075	.0033	-.151
<u>322</u>	.006	<u>.0012</u>	-.016	.031	.0016	-.067	.074	.0041	-.164
323	-.037	.0021	.091	-.017	.0017	.035	.022	.0027	-.058
324	.004	.0014	-.008	.029	.0015	-.060	.076	.0028	-.161
<u>325</u>	.019	<u>.0010</u>	.006	.039	.0013	-.042	.099	.0036	-.164
326	-.056	.0015	.125	-.032	.0008	.068	.016	.0007	-.061
327	.042	.0015	-.082	.071	.0027	-.142	.128	.0058	-.283
328	-.042	.0015	.082	-.021	.0009	.029	.020	.0019	-.069
329	-.038	.0015	.107	-.017	.0008	.045	.038	.0021	-.065
330	.056	.0015	-.125	.075	.0033	-.178	.118	.0084	-.281

TABLE V - PRINCIPAL AERODYNAMIC CHARACTERISTICS OF THE COMBINATIONS




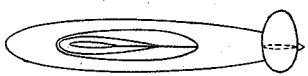
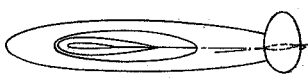
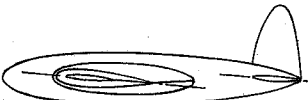
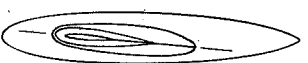


Diagrams representing combinations	Combination	Remarks	Longitudinal position d/c	Vertical position k/c	Angle of wing setting i_w (deg.)	Lift-curve slope (per degree) $\frac{A}{\alpha}$ A=6.86	Span efficiency factor e	$C_{D_{min}}$	$C_{L_{opt}}$	Aerodynamic-center-position x_o	C_{m_0}	Lift coefficient at interference bubble $C_{L_{ib}}$	$C_{L_{max}}$	
													Effective $R = 8.2 \times 10^6$	Effective $R = 3.7 \times 10^6$
Tapered N.A.C.A. 0018-09 airfoil with round fuselage														
	-	Wing alone	-	-	-	0.077	0.90	0.0093	0.00	0.020	0.000	A _{1.4}	C _{1.48}	C _{1.23}
	230	(From reference 2) Tapered fillets (Plaster finish)	0	0	0	.080	*.85	.0117	.00	.026	.000	A _{1.5}	C _{1.52}	C _{1.27}
	314	Tapered fillets. Vertical and horizontal tail surfaces. $i_s = 0^\circ$.	0	0	0	.086	*.85	.0128	*.02	*.100	.002	A _{1.7}	C _{1.73}	C _{1.47}
	315	$i_s = -4^\circ$; otherwise same as combination 314	0	0	0	.087	*.90	.0133	*.82	*.156	.102	A _{1.6}	C _{1.62}	C _{1.34}
	316	Tapered fillets. Tail surfaces with end plates. $i_s = 0^\circ$	0	0	0	.086	*.85	.0132	*.02	*.098	.001	A _{1.6}	C _{1.67}	C _{1.40}
	317	$i_s = -4^\circ$; otherwise same as combination 316	0	0	0	.087	*.90	.0134	*.75	*.122	.086	A _{1.6}	C _{1.62}	C _{1.33}
	318	Washed-out fillets. Vertical and horizontal tail surfaces. $i_s = 0^\circ$	0	0	4	.086	*.85	.0142	*.33	*.129	-.044	A _{1.4}	C _{1.42}	C _{1.38}
	319	Symmetrical tapered fillets	0	0	4	.080	*.85	.0117	.02	.027	-.021	A _{1.5}	C _{1.55}	C _{1.25}
	320	Same as combination 319 but with vertical and horizontal tail surfaces. $i_s = 0^\circ$	0	0	4	.087	*.85	.0132	*.29	*.115	-.033	A _{1.6}	C _{1.66}	C _{1.36}

Table V (continuation)

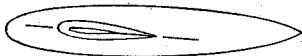

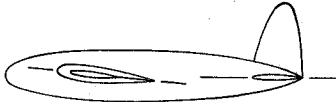




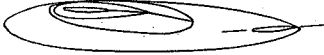
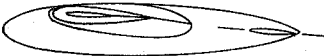

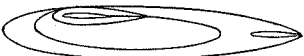


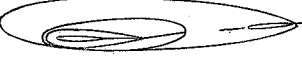

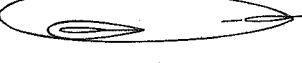


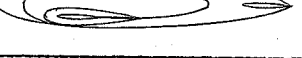
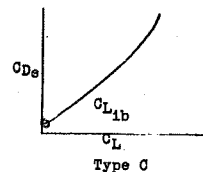
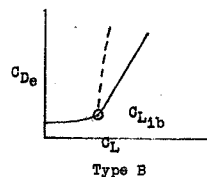
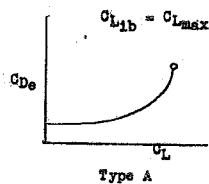
Diagrams representing combinations	Com- bina- tion	Remarks	Longi- tudinal posi- tion d/c	Verti- cal posi- tion k/c	Angle of wing set- ting i_w (deg)	Lift- curve slope (per degree) $A=6.86$	Span effi- ciency factor e	$C_{D_{min}}$	$C_{L_{opt}}$	Aerody- namic center- position x_0	C_{m_0}	Lift coef- ficient at interference bubble $C_{L_{ib}}$	$C_{L_{max}}$	
													Effec- tive $R = 8.2 \times 10^6$	Effec- tive $R = 3.7 \times 10^6$
Tapered N.A.C.A. 0018-09 airfoil with round fuselage														
	321		0	0	4	.080	.85	.0120	.02	.034	-.021	$A_{1.5}$	$C_{1.50}$	$a_{1.22}$
	322	Vertical and hori- zontal tail sur- faces. $i_s = 0^\circ$	0	0	4	.087	.85	.0133	-.32	-.116	-.039	$A_{1.6}$	$C_{1.67}$	$a_{1.35}$
	323	$i_s = -4^\circ$; other- wise same as com- bination 322	0	0	4	.086	.85	.0138	.51	-.110	.062	$A_{1.6}$	$C_{1.60}$	$a_{1.31}$
	324	Tail surfaces with end plates. $i_s = 0^\circ$	0	0	4	.086	.85	.0135	-.28	-.114	-.032	$A_{1.6}$	$C_{1.65}$	$a_{1.34}$
	325	Tapered fillets. Horizontal tail surfaces. $i_s = 0^\circ$	0	0	0	.086	.85	.0127	.06	-.087	.005	$A_{1.7}$	$C_{1.72}$	$a_{1.41}$
	306	(From reference 6) Tapered fillets	0	.22	0	.080	.85	.0122	-.02	.032	-.001	$A_{1.6}$	$C_{1.65}$	$a_{1.36}$
	312	(From reference 6) Tapered fillets. Horizontal tail surfaces. $i_s = 0^\circ$	0	.22	0	.087	.85	.0129	.14	-.133	.019	$A_{1.8}$	$C_{1.84}$	$a_{1.50}$
	326	$i_s = -4^\circ$; otherwise same as combination 312	0	.22	0	.085	.85	.0137	.77	-.166	.116	$A_{1.7}$	$C_{1.76}$	$a_{1.46}$
	327	$i_s = 4^\circ$; otherwise same as combination 312	0	.22	0	.086	.80	.0133	-.61	-.125	-.077	$A_{1.8}$	$C_{1.81}$	$a_{1.50}$
	308	(From reference 6) Straight-side jun- ctures	0	.22	0	.078	.85	.0118	-.03	.041	.010	$A_{1.5}$	$b_{1.58}$	$a_{1.27}$
	310	(From reference 6) Straight-side jun- ctures. Horizontal tail surfaces. $i_s = 0^\circ$	0	.22	0	.086	.85	.0128	.13	-.127	.016	$A_{1.7}$	$C_{1.75}$	$a_{1.46}$

Table V (conclusion)

Diagrams representing combinations	Combina- tion	Remarks	Longi- tudinal posi- tion d/c	Verti- cal posi- tion k/c	Angle of wing set- ting i_w (deg.)	Lift- curve slope (per degree) a $A=8.86$	Span effi- ciency factor e	$C_{D_{min}}$	$C_{L_{opt}}$	Aerody- namic center- position n_o	C_{m_0}	Lift coef- ficient at interference bubble $C_{L_{1b}}$	$C_{L_{max}}$	
													Effec- tive $R =$ $8.2 \times$ 10^6	Effec- tive $R =$ $3.7 \times$ 10^6
Tapered N.A.C.A. 0018-09 airfoil with round fuselage														
	307	(From reference 6) Tapered fillets	0	-.22	0	.081	^a .85	.0122	.02	.030	.001	^a 1.5	^a 1.57	^a 1.26
	313	(From reference 6) Tapered fillets. Horizontal tail surfaces. $i_s = 0^\circ$	0	-.22	0	.087	^a .85	.0129	^a -.15	^a -.127	-.019	^a 1.7	^c 1.72	^a 1.37
	328	$i_s = -4^\circ$; otherwise same as combination 313	0	-.22	0	.086	^a .85	.0133	^a .61	^a -.125	.077	^a 1.6	^c 1.66	^a 1.30
	187	(From reference 1)	0	-.22	0	.079	.85	.0124	-.02	.039	-.008	^b .9	^c 1.33	^a 1.14
	329	Horizontal tail surfaces. $i_s = -4^\circ$	0	-.22	0	.085	^a .90	.0139	^a .69	^a -.137	.095	^b 1.0	^c 1.42	^a 1.23
	330	$i_s = 4^\circ$; otherwise same as combination 313	0	-.22	0	.086	^a .80	.0137	^a -.77	^a -.166	-.115	^a 1.6	^c 1.74	^a 1.38
	309	(From reference 6) Straight-side junctures	0	-.22	0	.079	^a .85	.0118	.03	.041	-.010	^a 1.5	^c 1.50	^a 1.23
	311	(From reference 6) Straight-side jun- ctures. Horizontal tail surfaces. $i_s = 0^\circ$	0	-.22	0	.086	^a .85	.0128	^a -.13	^a -.125	-.016	^a 1.6	^c 1.66	^a 1.40

Letters refer to types of drag curves associated with the interference bubble as follows: ^a Letters refer to condition at maximum lift as follows: ^a reasonably steady at $C_{L_{max}}$; ^b small loss of lift beyond $C_{L_{max}}$; ^c large loss of lift beyond $C_{L_{max}}$ and uncertain value of $C_{L_{max}}$.



^a Poor agreement in high-speed range.

^a Poor agreement over whole range.

^a Poor agreement in high-lift range.

^a $C_{D_{min}}$ at $C_{m_0/4} = 0$ for combinations with tail surfaces.

^a $n_o = dC_{m_0/4} / dC_L$ at $C_{m_0/4} = 0$ for combinations with tail surfaces.

FIGURE LEGENDS

Figure 1.- Combination 314 showing elliptical tail surfaces.

Figure 2.- Combination 316 showing rectangular tail surfaces with end plates.

Figure 3.- Combination 329 showing unfilleted juncture.

	x (in.)	y ₁ (in.)	y ₂ (in.)
(a) Elliptical tail surface.			
Fin area: 11.46 sq.in.;	0	1.403	--
0.076 of wing area.	1.0	1.381	--
Area horizontal surfaces	2.0	1.308	1.598
(including 4.08 sq.in.	3.0	1.177	1.439
in fuselage): 27.00 sq.in.;	4.0	.965	1.179
0.18 of wing area.	5.0	.588	.718
	5.51	0	0
	z (in.)	w ₁ (in.)	w ₂ (in.)
(b) Tail surface with end plate.			
Fin (end plates) area:	0	0	0
17.88 sq.in.; 0.119 of	.240	.728	.596
wing area.	1.240	1.378	1.126
Area horizontal surfaces	2.240	1.412	1.154
(including 3.70 sq.in. in	3.240	1.178	.964
fuselage): 21.02 sq.in.;	4.240	.416	.340
0.14 of wing area.	4.352	0	0

Figure 4.- Details of the tail surfaces - N.A.C.A. 0009 sections.

Figure 5.- Characteristics of midwing combinations with various tail surfaces. Tapered N.A.C.A. 0018-09 airfoil and round fuselage; $k/c = 0$; $i_w = 0^\circ$.

Figure 6.- Effects of tail setting on the characteristics of high-wing combinations. Tapered N.A.C.A. 0018-09 airfoil and round fuselage; $k/c = 0.22$; $i_w = 0^\circ$.

Figure 7.- Effects of tail setting on the characteristics of low-wing combinations. Tapered N.A.C.A. 0018-09 airfoil and round fuselage; $k/c = -0.22$; $i_w = 0^\circ$.

Figure 8.-- Effects of wing vertical position. Tapered N.A.C.A. 0018-09 airfoil and round fuselage; $i_w = 0^\circ$; $i_s = 0^\circ$.

Figure 9.-- Effects of fillets on the characteristics of low-wing combinations. Tapered N.A.C.A. 0018-09 airfoil and round fuselage; $k/c = -0.22$; $i_w = 0^\circ$; $i_s = -4^\circ$.

Figure 10.-- Effects of wing setting on the characteristics of midwing combinations. Tapered N.A.C.A. 0018-09 airfoil and round fuselage; $k/c = 0$; $i_s = 0^\circ$.

Figure 11.-- Comparison of experimental and predicted values of the downwash angle at the tail. $A = 6.86$.

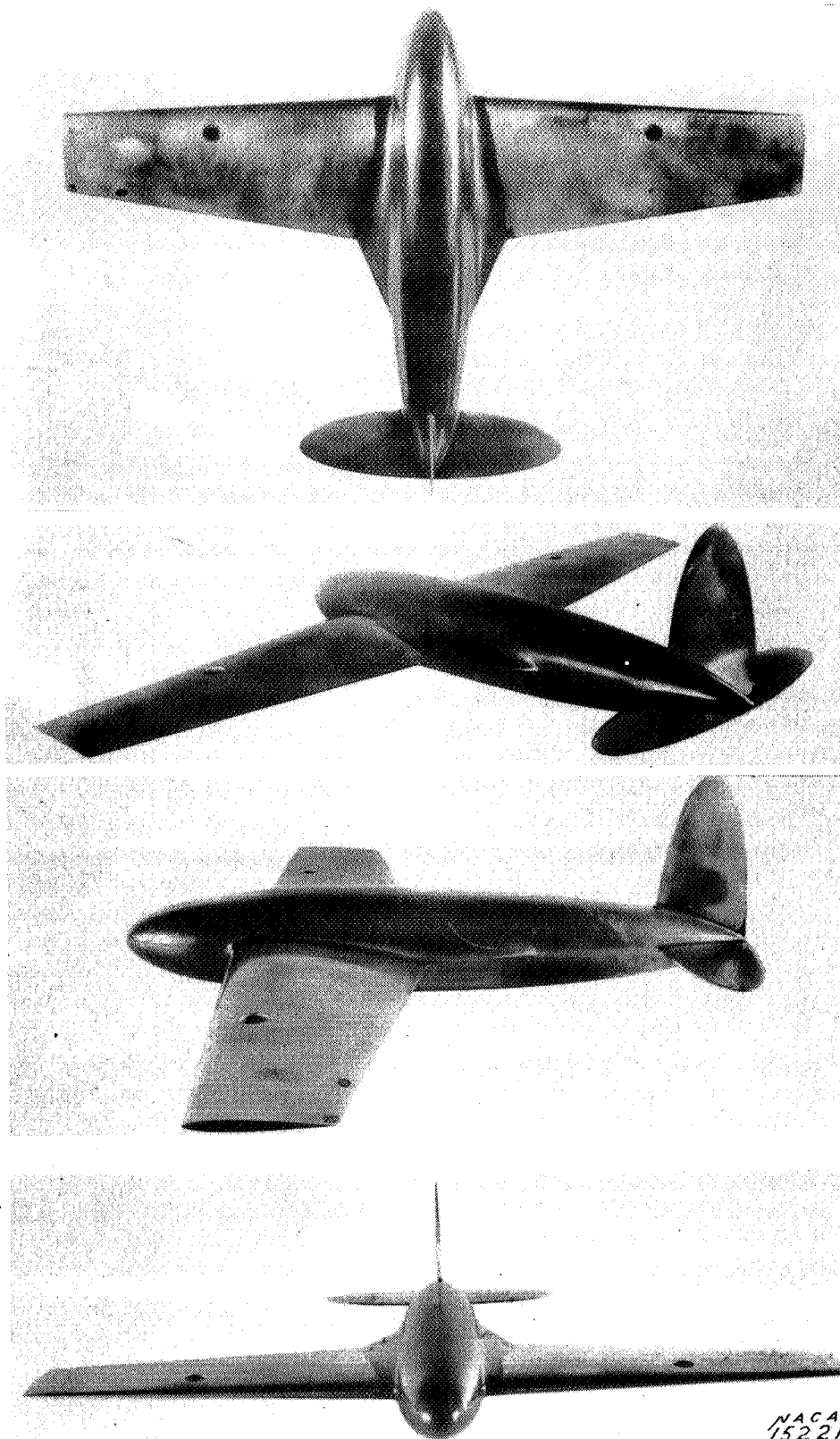


Figure 1.- Combination 314 showing elliptical tail surfaces.

NACA
15221

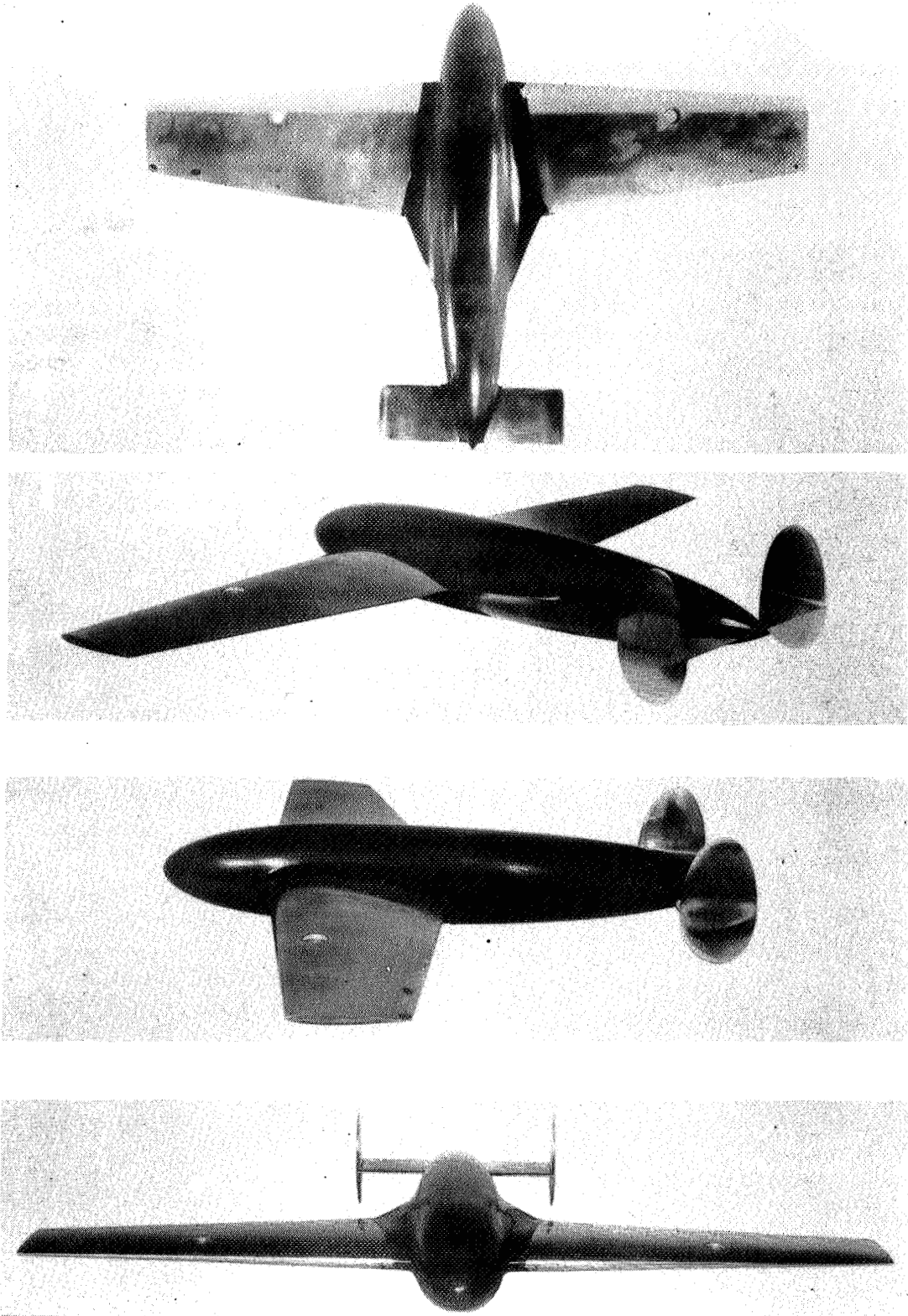


Figure 2.- Combination 316 showing rectangular tail surface with end-plates.

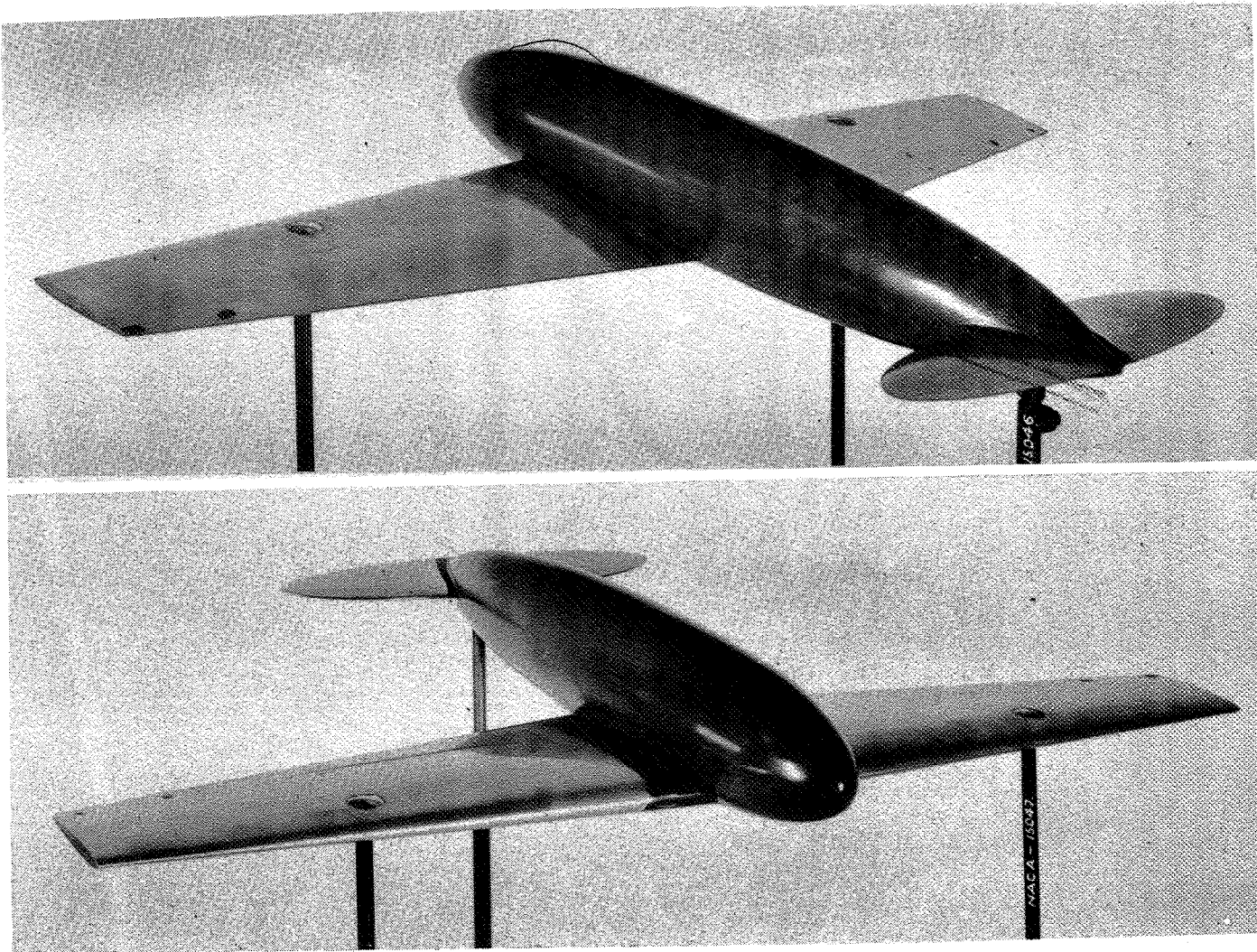
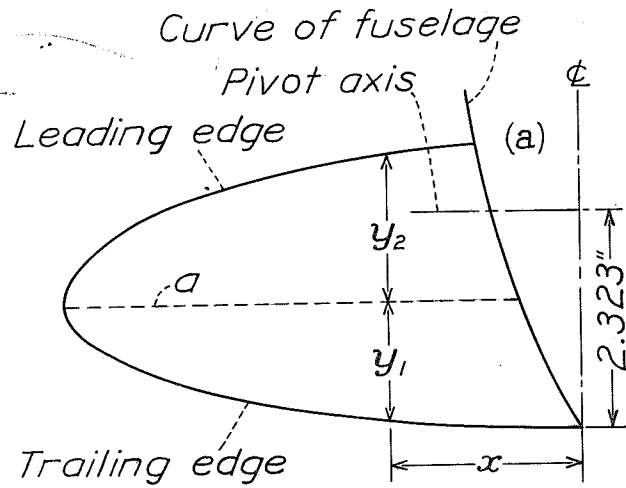
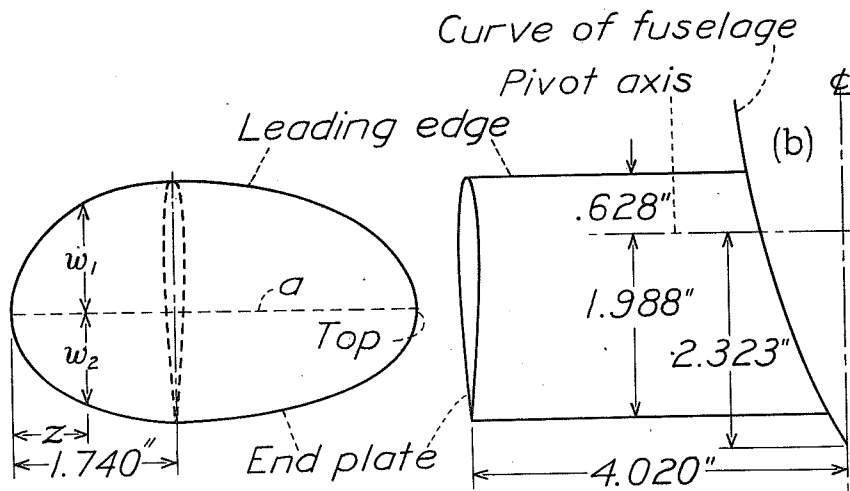


Figure 3.- Combination 329 showing unfilleted juncture.



a, (Line of points .45c from T.E.)



a, (Line of points .45c from T.E.)

Figure 4.

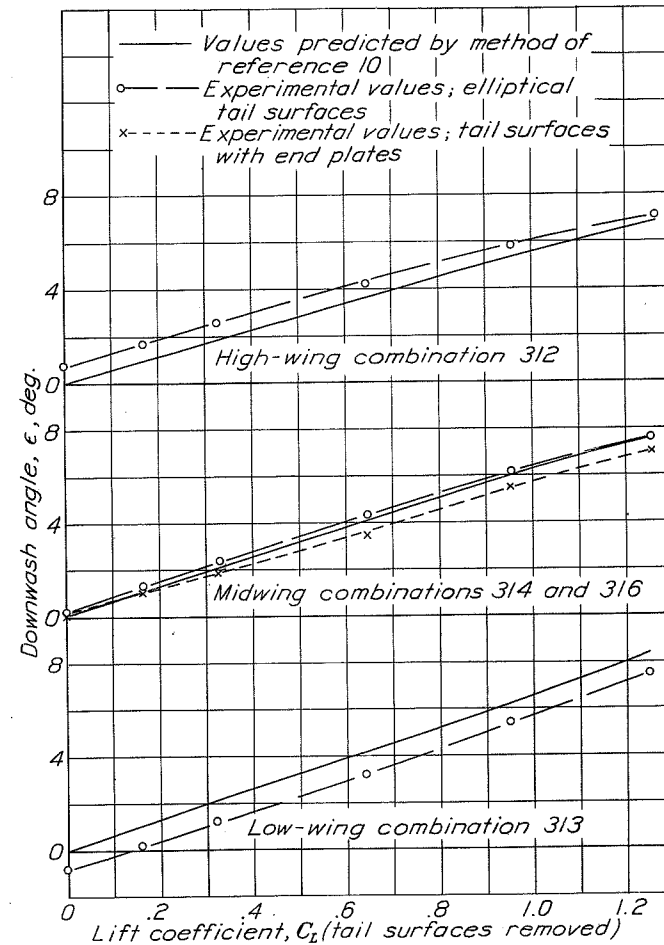


Figure 11.

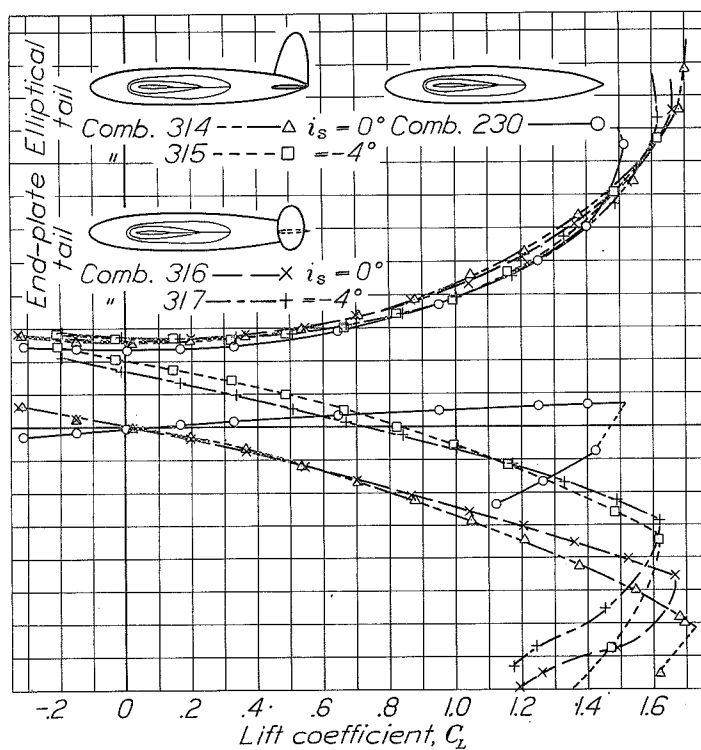


Figure 5.

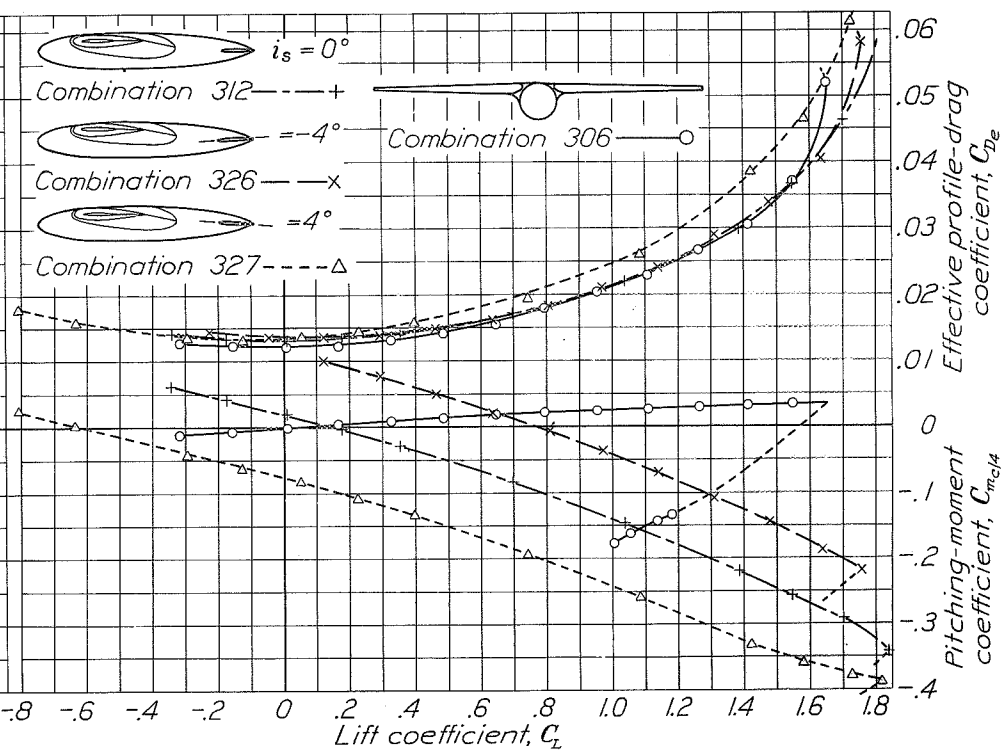
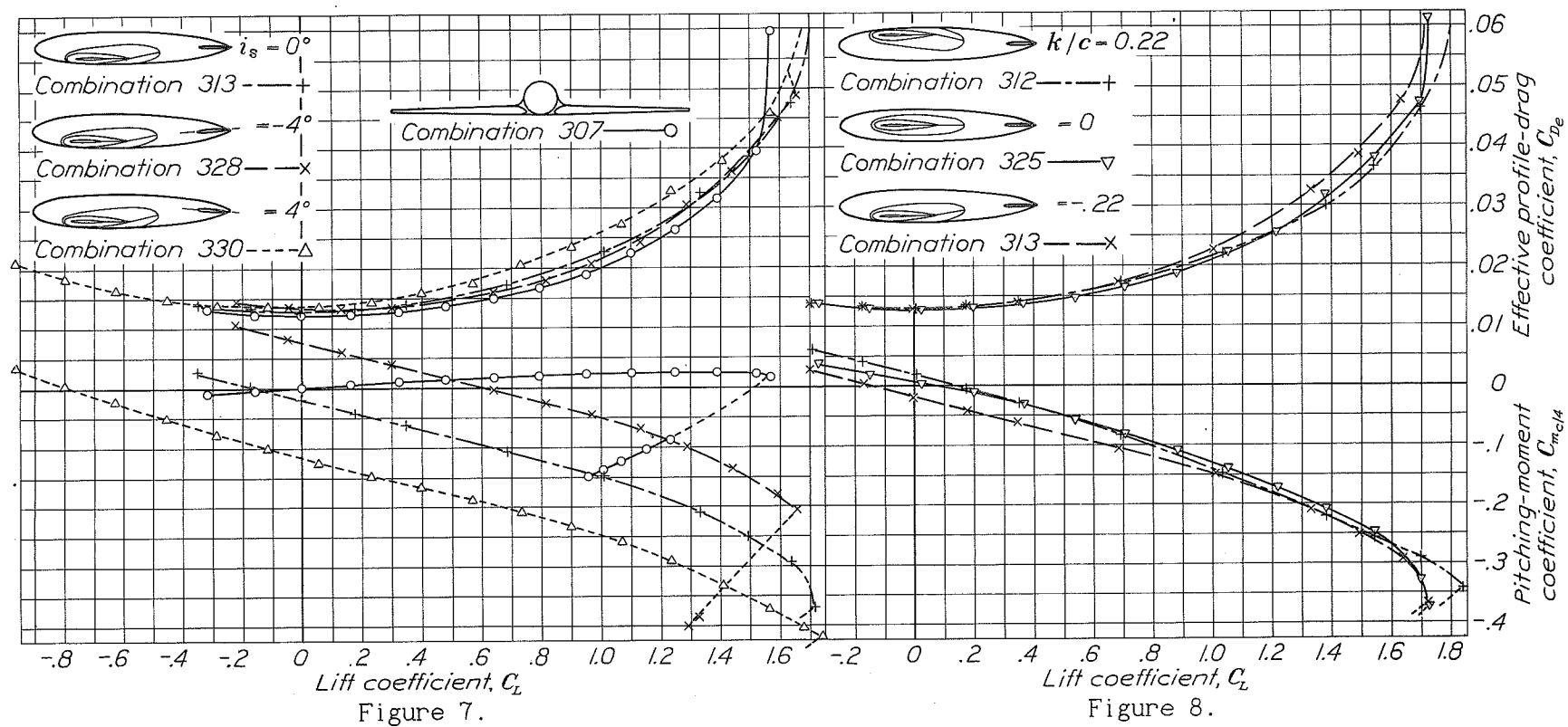
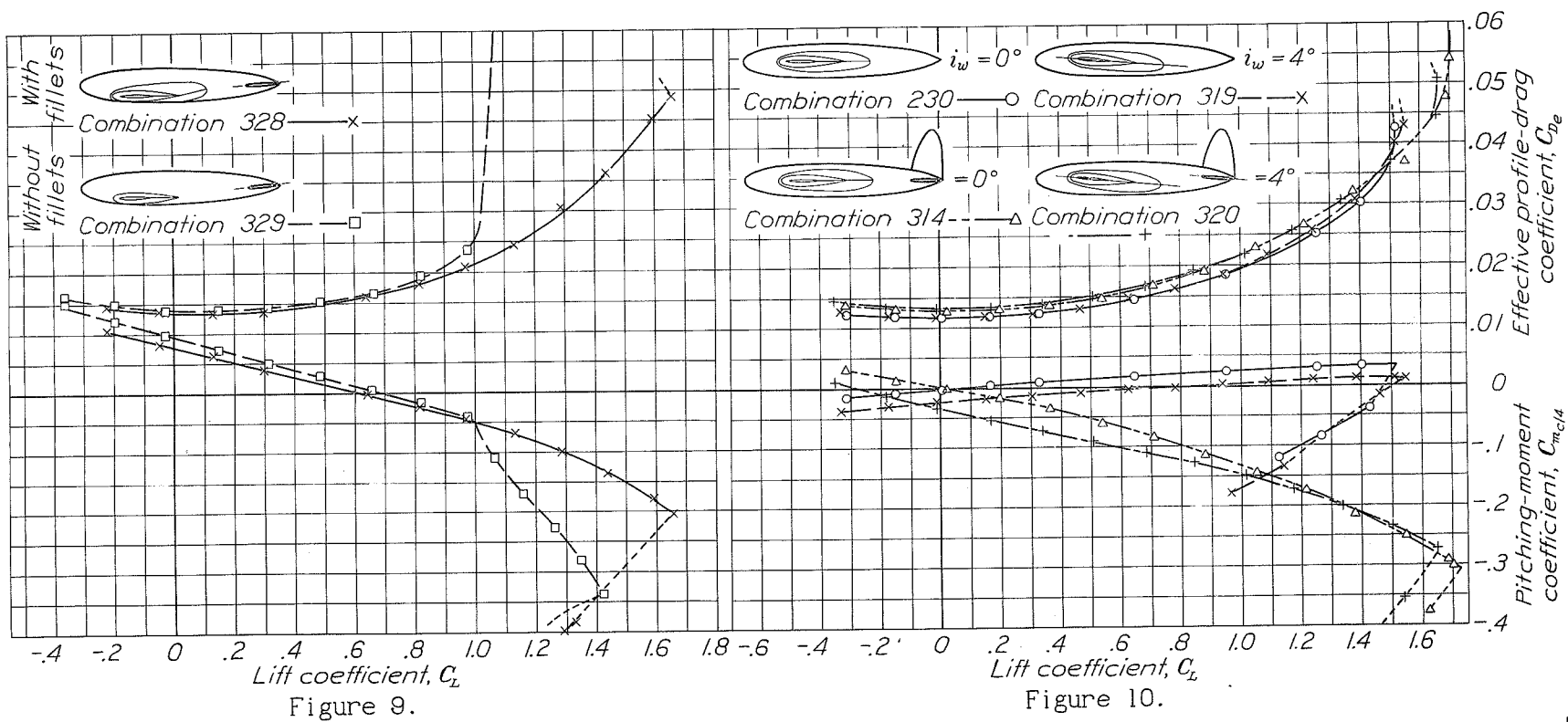


Figure 6.





Figs. 9, 10